International Journal of Solids and Structures 48 (2011) 2743–2754

Contents lists available at ScienceDirect

International Journal of Solids and Structures

journal homepage: www.elsevier.com/locate/ijsolstr

Indentation responses of piezoelectric films ideally bonded to an elastic substrate

J.H. Wang [a], C.Q. Chen [b,*]

[a] MOE Key Laboratory for Strength and Vibration, School of Aerospace, Xi'an Jiaotong University, Xi'an 710049, PR China
[b] Department of Engineering Mechanics, AML & CNMM, Tsinghua University, Beijing 100084, PR China

ARTICLE INFO

Article history:
Received 7 February 2011
Received in revised form 15 April 2011
Available online 22 June 2011

Keywords:
Indentation
Piezoelectric film
Elastic substrate
Numerical analysis
Finite element method

ABSTRACT

The influences of elastic substrate on the indentation force, contact radius, electric potential and electric charge responses of piezoelectric film/substrate systems are investigated by the integral transform method. The film is assumed to be ideally bonded to the substrate and the contact interaction between the indenter and the film is assumed to be frictionless, with three kinds of axisymmetric insulating and conducting indenters (i.e., punch, cone and sphere) considered. Obtained results show that when the ratio of the contact radius to the film thickness is close to zero, the influences of the elastic substrate disappear and the indentation behaviors converge to the piezoelectric half space solutions while the indentation responses approach the corresponding ones of elastic half space as the ratio gets to infinity. The transition between the piezoelectric and the elastic half space indentation solutions for the film/substrate system is quantified in terms of the film thickness and the elasticity of the substrate. Finite element analysis on an insulating sphere indentation is conducted to verify the numerical calculations and good agreement is observed. The obtained results are believed to be useful for developing experimental techniques to extract the material properties of piezoelectric film/substrate systems.

1. Introduction

Piezoelectric materials in the form of film bonded to substrate are widely used in microelectromechanical systems (MEMS) as actuators and sensors, due to their attractive mechanical and electric coupling effects (Mason, 1950; Uchino, 1997). The film thickness can range from a few nanometers to several millimeters. To measure the mechanical and electric properties of the piezoelectric materials used in applications that they are prone to contact in thin-film and bulk forms, the instrumented indentation techniques, which are based on the methods developed by Oliver and Pharr (1992, 2004) originally for elastic half space, can offer a powerful tool (Bahr et al., 1999; Sridhar et al., 1999; Zheng et al., 2003; Delobelle et al., 2004; Rar et al., 2006). However, successful application of the techniques to piezoelectric films depends to a large extent upon the availability of reliable closed-form exact or approximate indentation models.

Indentation responses of piezoelectric materials, when compared to those of elastic materials, are more complicated owing to the directional dependence and mechanical–electrical coupled characteristics of the materials. A number of theoretical and experimental studies on this subject are available. Using the Hankel transformation method, Matysiak (1985) obtained the solution for a linear piezoelectric half space penetrated by a rigid conducting punch. Following the same methodology, Giannakopoulos and Suresh (1999) investigated the axisymmetric indentation of a piezoelectric half space pressed by three different types of insulating and conducting indenters (i.e., punch, cone and sphere) within the context of fully coupled, transversely isotropic models. Yang (2008) presented a closed-form solution of the axisymmetric indentation for a semi-infinite transverse isotropic piezoelectric material by a rigid-conducting indenter of arbitrary-axisymmetric profile. Effective contact stiffness and piezoelectric constant were obtained. Alternatively, the potential theory technique was adopted by Wang and Zheng (1995), Chen and Ding (1999), Chen et al. (1999), Ding et al. (2000), and Kalinin et al. (2004) to derive analytical indentation solutions of a transversely isotropic piezoelectric half space. Karapetian et al. (2009) studied the piezoelectric indentation of flat and non-flat indenters with arbitrary form, under normal force (centrally or non-centrally applied) and electric charge distributions prescribed at the base.

Similar to successful implementation of traditional indentation of elastic materials (Busby et al., 2005), experimental studies on piezoelectric materials were conducted by many researchers. The indentation force response of lead zirconate and barium titanate piezoelectric ceramics to spherical micro-indentation was experimentally investigated by Ramamurty et al. (1999). The electric responses during indentation of piezoelectric materials was studied experimentally by Sridhar et al. (1999) and the experimental results were larger than the theoretical prediction, which was likely due to the occurrence of inelastic deformation and the time-dependence of the piezoelectric interaction. Delobelle et al. (2004) used the traditional indentation method to measure the

* Corresponding author. Tel./fax: +86 10 62783488.
E-mail address: chencq@tsinghua.edu.cn (C.Q. Chen).

0020-7683/$ - see front matter © 2011 Elsevier Ltd. All rights reserved.
doi:10.1016/j.ijsolstr.2011.05.023

effective indentation modulus of PZT films. Similar to the technique of the piezoresponse force microscopy (PFM) (Birk et al., 1991; Zavala et al., 1997; Zhao et al., 2004), Rar et al. (2006) assessed the piezoresponse of polycrystalline lead zirconate titanate and $BaTiO_3$ piezoelectric ceramics by applying an oscillating voltage between the indenter-tip and the back-electrode.

However, it is noted that all the aforementioned studies on indentation mainly focus on the half space case. For film/substrate systems, the corresponding indentation responses are much more complicated. General speaking, as a rule of thumb, when the ratio of contact radius to film thickness is less than one tenth, the effects of the substrate on the indentation responses can be neglected and the solutions for indentation of half space apply (e.g., Johnson, 1985; Oliver and Pharr, 1992). On the other hand, when the ratio of the contact radius to the film thickness is large enough, simplified approximate solutions can be obtained by employing Johnson's assumption of "plane sections remain plane after compression" (Johnson, 1985) and other methods (Yang, 2003; Ning et al., 2006; Wang et al., 2008b). For intermediate values of film thickness, an important and difficult issue to be addressed is to quantify the effects of the film thickness and the substrate on the indentation responses. A number of studies on the elastic film/substrate system have been conducted for such purpose (Doerner and Nix, 1986; King, 1987; Gao et al., 1992; Mencik et al., 1997; Yu, 2001; Saha and Nix, 2002; Yang, 2003; Chen et al., 2005; Gao et al., 2008). For indentations of piezoelectric film/elastic substrate, both experimental and theoretical studies on piezoelectric thin films (Christman et al., 1998; Bahr et al., 1999; Zheng et al., 2003; Delobelle et al., 2004) and multilayered piezoelectric media (Wang et al., 2002; Wang and Han, 2006) have been reported. Wang et al. (2008b) conducted a systematic theoretical analysis on the axisysmetric indentation of piezoelectric film/substrate system by three ideal insulating and conducting indenters. Three cases of half space, thin film with finite thickness and ultra-thin film were considered. They proposed corresponding semi-empirical indentation responses formulae which were thought to be useful for developing experimental indentation techniques to extract the material properties of piezoelectric films. The electromechanical behaviors of a finite piezoelectric ceramic layer indented by a flat punch were also investigated by another group (Wang et al., 2008a). Nevertheless, in their studies the substrate was assumed to be rigid and it is only a rough approximation of the case of soft film on rather hard substrate. In reality, however, the substrate may not be regarded as rigid and its elasticity could have big influence on the indentation responses. So far, the indentation of a piezoelectric film on an elastic substrate is rarely mentioned or studied. It is therefore desirable to carry out a systematic theoretic research to explore the effects of the elastic substrate on the indentation responses.

In what follows, this paper is concerned with the electromechanical indentation responses of the piezoelectric film perfectly bonded to an elastic substrate with different Young's moduli and Poisson's ratios. Different types of indenter geometry and different electrical boundary conditions (perfectly insulating and perfectly conducting) are considered. The frictionless condition for the contact between the indenter and the film and ideally bonding condition between the film and the substrate are adopted. The focus is placed on quantifying the influences of the substrate elasticity on the indentation responses of the piezoelectric film elastic substrate system.

2. Fundamental formulae

2.1. Models

The problem to be considered is a transversely isotropic piezoelectric film (Chen and Ding, 1999; Giannakopoulos and Suresh, 1999; Karapetian et al., 2002; Chen and Yu, 2005) ideally bonded

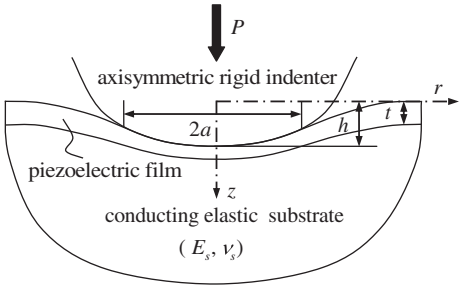

Fig. 1. Illustration of the axisymmetric indentation of a piezoelectric film bonded to a conducting elastic substrate with Young's modulus E_s and Poisson's ratio ν_s.

to an isotropic elastic substrate with Young's modulus E_s and Poisson's ratio ν_s and penetrated by an axisymmetric rigid indenter. The cylindrical polar coordinate system (r,θ,z) is introduced and the piezoelectric film is isotopic in the $(r-\theta)$ plane (Fig. 1), where P, h and a denote the indentation force, depth, and contact radius, respectively, and t represents the film thickness. Three different types of rigid indenters are considered: a punch with radius a, a cone with included semi-apex angle Θ, and a sphere with radius R. The contact between the indenters and the film is assumed to be frictionless. It is noted that the coordinate system for the elastic substrate is (r,θ,z') with $z'=z-t$.

2.2. General solutions

The governing equations in terms of the displacement components u_r and u_z and the electric potential ϕ for the piezoelectric media can be expressed as

$$\begin{aligned}
&c_{11}\left(\frac{\partial^2 u_r}{\partial r^2}+\frac{1}{r}\frac{\partial u_r}{\partial r}-\frac{u_r}{r^2}\right)+c_{44}\frac{\partial^2 u_r}{\partial z^2}+(c_{13}+c_{44})\frac{\partial^2 u_z}{\partial r\partial z}\\
&\qquad+(e_{31}+e_{15})\frac{\partial^2\phi}{\partial r\partial z}=0,\\
&(c_{13}+c_{44})\frac{\partial}{\partial z}\left(\frac{\partial u_r}{\partial r}+\frac{u_r}{r}\right)+c_{44}\left(\frac{\partial^2 u_z}{\partial r^2}+\frac{1}{r}\frac{\partial u_z}{\partial r}\right)+c_{33}\frac{\partial^2 u_z}{\partial z^2}\\
&\qquad+e_{15}\left(\frac{\partial^2\phi}{\partial r^2}+\frac{1}{r}\frac{\partial\phi}{\partial r}\right)+e_{33}\frac{\partial^2\phi}{\partial z^2}=0\\
&(e_{15}+e_{31})\frac{\partial}{\partial z}\left(\frac{\partial u_r}{\partial r}+\frac{u_r}{r}\right)+e_{15}\left(\frac{\partial^2 u_z}{\partial r^2}+\frac{1}{r}\frac{\partial u_z}{\partial r}\right)+e_{33}\frac{\partial^2 u_z}{\partial z^2},\\
&\qquad-\in_{11}\left(\frac{\partial^2\phi}{\partial r^2}+\frac{1}{r}\frac{\partial\phi}{\partial r}\right)-\in_{33}\frac{\partial^2\phi}{\partial z^2}=0,
\end{aligned}\tag{1}$$

where c_{ij}, e_{ij} and $\in_{ij}$ are respectively the elastic, piezoelectric and dielectric constants. Considering the axisymmetric nature of the considered problems, the general indentation solutions of Eq. (1) through the Hankel transformation technique are given as follows (Wang et al., 2008b)

$$\begin{aligned}
u_r(r,z)=\int_0^\infty\{&\left[\alpha_1A_1(\xi)e^{-k_1\xi z}+(\alpha_{21}A_2(\xi)-\alpha_{22}A_3(\xi))e^{-\delta\xi z}\cos(\omega\xi z)\right.\\
&\left.+(\alpha_{22}A_2(\xi)+\alpha_{21}A_3(\xi))e^{-\delta\xi z}\sin(\omega\xi z)\right]\\
&+\left[\alpha_3A_4(\xi)e^{k_1\xi z}+(\alpha_{41}A_5(\xi)-\alpha_{42}A_6(\xi))e^{\delta\xi z}\cos(\omega\xi z)\right.\\
&\left.-(\alpha_{42}A_5(\xi)+\alpha_{41}A_6(\xi))e^{\delta\xi z}\sin(\omega\xi z)\right]\}\xi J_1(\xi r)d\xi,
\end{aligned}\tag{2}$$

$$\begin{aligned}
u_z(r,z)=\int_0^\infty\{&\left[\beta_1A_1(\xi)e^{-k_1\xi z}+(\beta_{21}A_2(\xi)-\beta_{22}A_3(\xi))e^{-\delta\xi z}\cos(\omega\xi z)\right.\\
&\left.+(\beta_{22}A_2(\xi)+\beta_{21}A_3(\xi))e^{-\delta\xi z}\sin(\omega\xi z)\right]\\
&+\left[\beta_3A_4(\xi)e^{k_1\xi z}+(\beta_{41}A_5(\xi)-\beta_{42}A_6(\xi))e^{\delta\xi z}\cos(\omega\xi z)\right.\\
&\left.-(\beta_{42}A_5(\xi)+\beta_{41}A_6(\xi))e^{\delta\xi z}\sin(\omega\xi z)\right]\}\xi J_0(\xi r)d\xi,
\end{aligned}\tag{3}$$

$$\phi(r,z)=\int_0^\infty\{[\gamma_1A_1(\xi)e^{-k_1\xi z}+(\gamma_{21}A_2(\xi)-\gamma_{22}A_3(\xi))e^{-\delta\xi z}\cos(\omega\xi z)+(\gamma_{22}A_2(\xi)+\gamma_{21}A_3(\xi))e^{-\delta\xi z}\sin(\omega\xi z)]+[\gamma_3A_4(\xi)e^{k_1\xi z}+(\gamma_{41}A_5(\xi)-\gamma_{42}A_6(\xi))e^{\delta\xi z}\cos(\omega\xi z)-(\gamma_{42}A_5(\xi)+\gamma_{41}A_6(\xi))e^{\delta\xi z}\sin(\omega\xi z)]\}\xi J_0(\xi r)d\xi, \tag{4}$$

where $A_1(\xi)\sim A_6(\xi)$ are unknown coefficients to be determined by boundary conditions and α, β, and γ are coefficients related with the material properties which can be found in Wang et al. (2008b).

On the contact surface ($z=0$), the displacement components and electric potential are given by

$$u_r(r,0)=\int_0^\infty[(\alpha_1A_1(\xi)+\alpha_{21}A_2(\xi)-\alpha_{22}A_3(\xi))+(\alpha_3A_4(\xi)+\alpha_{41}A_5(\xi)-\alpha_{42}A_6(\xi))]\xi J_1(\xi r)d\xi, \tag{5}$$

$$u_z(r,0)=\int_0^\infty[(\beta_1A_1(\xi)+\beta_{21}A_2(\xi)-\beta_{22}A_3(\xi))+(\beta_3A_4(\xi)+\beta_{41}A_5(\xi)-\beta_{42}A_6(\xi))]\xi J_0(\xi r)d\xi, \tag{6}$$

$$\phi(r,0)=\int_0^\infty[(\gamma_1A_1(\xi)+\gamma_{21}A_2(\xi)-\gamma_{22}A_3(\xi))+(\gamma_3A_4(\xi)+\gamma_{41}A_5(\xi)-\gamma_{42}A_6(\xi))]\xi J_0(\xi r)d\xi. \tag{7}$$

Correspondingly, the stresses and electric displacement are

$$\sigma_{zr}(r,0)=\int_0^\infty[(l_1A_1(\xi)+l_2A_2(\xi)-l_3A_3(\xi))+(l_4A_4(\xi)+l_5A_5(\xi)-l_6A_6(\xi))]\xi^2J_1(\xi r)d\xi, \tag{8}$$

$$\sigma_{zz}(r,0)=\int_0^\infty[(m_1A_1(\xi)+m_2A_2(\xi)-m_3A_3(\xi))+(m_4A_4(\xi)+m_5A_5(\xi)-m_6A_6(\xi))]\xi^2J_0(\xi r)d\xi, \tag{9}$$

$$D_z(r,0)=\int_0^\infty[(n_1A_1(\xi)+n_2A_2(\xi)-n_3A_3(\xi))+(n_4A_4(\xi)+n_5A_5(\xi)-n_6A_6(\xi))]\xi^2J_0(\xi r)d\xi. \tag{10}$$

On the interface between the film and the substrate ($z=t$), one can obtain

$$u_r(r,t)=\int_0^\infty[(E_\alpha A_1(\xi)+F_\alpha A_2(\xi)-G_\alpha A_3(\xi))+(H_\alpha A_4(\xi)+I_\alpha A_5(\xi)-J_\alpha A_6(\xi))]\xi J_1(\xi r)d\xi, \tag{11}$$

$$u_z(r,t)=\int_0^\infty[(E_\beta A_1(\xi)+F_\beta A_2(\xi)-G_\beta A_3(\xi))+(H_\beta A_4(\xi)+I_\beta A_5(\xi)-J_\beta A_6(\xi))]\xi J_0(\xi r)d\xi, \tag{12}$$

$$\phi(r,t)=\int_0^\infty[(E_\gamma A_1(\xi)+F_\gamma A_2(\xi)-G_\gamma A_3(\xi))+(H_\gamma A_4(\xi)+I_\gamma A_5(\xi)-J_\gamma A_6(\xi))]\xi J_0(\xi r)d\xi, \tag{13}$$

$$\sigma_{zr}(r,t)=\int_0^\infty[(o_1A_1(\xi)+o_2A_2(\xi)-o_3A_3(\xi))+(o_4A_4(\xi)+o_5A_5(\xi)-o_6A_6(\xi))]\xi^2J_1(\xi r)d\xi, \tag{14}$$

$$\sigma_{zz}(r,t)=\int_0^\infty[(q_1A_1(\xi)+q_2A_2(\xi)-q_3A_3(\xi))+(q_4A_4(\xi)+q_5A_5(\xi)-q_6A_6(\xi))]\xi^2J_0(\xi r)d\xi, \tag{15}$$

where the constants l_i, m_i, n_i, o_i, q_i and E_α, F_α, G_α, H_α, I_α, and J_α are defined in the Appendix A .

For the elastic substrate, the governing group Eq. (1) reduces to

$$\frac{2(1-\nu_s)}{1-2\nu_s}\left(\frac{\partial^2u_r^s}{\partial r^2}+\frac{1}{r}\frac{\partial u_r^s}{\partial r}-\frac{u_r^s}{r^2}\right)+\frac{\partial^2u_r^s}{\partial z'^2}+\frac{1}{1-2\nu_s}\frac{\partial^2u_{z'}^s}{\partial r\partial z'}=0$$

$$\frac{1}{1-2\nu_s}\frac{\partial}{\partial z'}\left(\frac{\partial u_r^s}{\partial r}+\frac{u_r^s}{r}\right)+\frac{\partial^2u_{z'}^s}{\partial r^2}+\frac{1}{r}\frac{\partial u_{z'}^s}{\partial r}+\frac{2(1-\nu_s)}{1-2\nu_s}\frac{\partial^2u_{z'}^s}{\partial z'^2}=0, \tag{16}$$

where the script "s" denotes the substrate. Applying the same method as that for the piezoelectric film, the following general solutions for the elastic substrate are obtained

$$u_r^s(r,z')=\int_0^\infty[M_1(\xi)\xi z'-M_1(\xi)(3-4\nu_s)+M_2(\xi)]\xi e^{-\xi z'}J_1(\xi r)d\xi, \tag{17}$$

$$u_{z'}^s(r,z')=\int_0^\infty[M_1(\xi)\xi z'+M_2(\xi)]\xi e^{-\xi z'}J_0(\xi r)d\xi \tag{18}$$

and the corresponding stress components are

$$\sigma_{rz'}^s(r,z')=\frac{E_s}{1+\nu_s}\int_0^\infty[-M_1(\xi)\xi z'+2M_1(\xi)(1-\nu_s)-M_2(\xi)]\xi^2e^{-\xi z'}J_1(\xi r)d\xi, \tag{19}$$

$$\sigma_{z'z'}^s(r,z')=\frac{E_s}{1+\nu_s}\int_0^\infty[(1-2\nu)M_1(\xi)-M_1(\xi)\xi z'-M_2(\xi)]\xi^2e^{-\xi z'}J_0(\xi r)d\xi,$$

where $M_1(\xi)$ and $M_2(\xi)$ are unknowns to be determined from the boundary conditions.

On the interface between the film and the substrate ($z=t$, that is $z'=0$), we have

$$u_r^s(r,0)=\int_0^\infty[-M_1(\xi)(3-4\nu_s)+M_2(\xi)]\xi J_1(\xi r)d\xi \tag{21}$$

$$u_{z'}^s(r,0)=\int_0^\infty M_2(\xi)\xi J_0(\xi r)d\xi, \tag{22}$$

$$\sigma_{rz'}^s(r,0)=\frac{E_s}{1+\nu_s}\int_0^\infty[2(1-\nu_s)M_1(\xi)-M_2(\xi)]\xi^2J_1(\xi r)d\xi, \tag{23}$$

$$\sigma_{z'z'}^s(r,0)=\frac{E_s}{1+\nu_s}\int_0^\infty[(1-2\nu_s)M_1(\xi)-M_2(\xi)]\xi^2J_0(\xi r)d\xi. \tag{24}$$

2.3. Boundary conditions

At $z=0$, within the contact area ($r\leqslant a$), the downward displacement u_z is specified in accordance with the indenter profile $f(r)$, as

$$u_z(r,0)=h-f(r) \tag{25}$$

with

$$f(r)=\begin{cases}0 & (0\leqslant r\leqslant a)\quad\text{(punch)},\\ r\cot\Theta & (0\leqslant r\leqslant a)\quad\text{(cone)},\\ r^2/(2R) & (0\leqslant r\leqslant a)\quad\text{(sphere)},\end{cases} \tag{26}$$

where it is assumed for the sphere indenter that $a\ll R$. Outside the contact area the normal stress must be zero

$$\sigma_{zz}(r,0)=0 \quad (r>a). \tag{27}$$

Since only frictionless contact is considered, one has

$$\sigma_{rz}(r,0)=0 \quad (r\geqslant 0). \tag{28}$$

The following electric boundary condition is prescribed

$$D_z(r,0)=0 \quad (r\geqslant 0) \tag{29}$$

for insulating indenters and

$$\begin{aligned}&\phi(r,0)=\phi_1 \quad (0\leqslant r\leqslant a),\\ &D_z(r,0)=0 \quad (r>a).\end{aligned} \tag{30}$$

for conducting indenters, where ϕ_1 is the prescribed indentation electric potential.

At $z=t$, that is $z'=0$, because of the deformation of the elastic substrate, the displacement components u_r and u_z are no longer zero, the following boundary conditions are presented

$$\{u_r \quad u_z \quad \sigma_{rz} \quad \sigma_{zz}\}=\{u_r^s \quad u_{z'}^s \quad \sigma_{rz'}^s \quad \sigma_{z'z'}^s\}. \tag{31}$$

The elastic substrate is assumed to be conducting, so

$$\phi(r,t)=0 \quad (r\geqslant 0) \tag{32}$$

Note that the foregoing boundary conditions are ideal. For any imperfect boundary conditions (e.g., the partly insulating and partly conducting condition by charge leaking), the following analysis no longer applies.

2.4. Dual integral equations

Applying the general solutions in Section 2.2 into the boundary conditions presented in the above section, we have the following linear group equations for the insulating indenter case,

Table 1
Indentation responses of isotropic elastic half space indented by three kinds of indenters (i.e., Punch, Cone and Sphere) where the subscript "*eh*" denotes elastic half space.

Quantity	Punch	Cone	Sphere
a_{eh}	constant	$\frac{2}{\pi}h\tan\Theta$	$\sqrt{Rh}$
P_{eh}	$\frac{2E}{(1-\nu^2)}ah$	$\frac{2E}{\pi(1-\nu^2)}h^2\tan\Theta$	$\frac{4E}{3(1-\nu^2)}R^{1/2}h^{3/2}$
$\phi_{eh}(r,0)$	0	0	0
Q_{eh}	0	0	0

Table 2
Material properties for PZT-4.

Elastic coefficients (GPa)				
c_{11}	c_{12}	c_{13}	c_{33}	c_{44}
139.00	77.80	74.30	115.00	25.60
Piezoelectric coefficients(C/m^2)			Dielectric constants(10^{-9}F/m)	
e_{31}	e_{33}	e_{15}	$\in_{11}$	$\in_{33}$
−5.20	15.10	12.70	6.461	5.620

$$\begin{pmatrix} l_1 & l_2 & l_3 & l_4 & l_5 & l_6 & 0 & 0\\ n_1 & n_2 & n_3 & n_4 & n_5 & n_6 & 0 & 0\\ E_\alpha & F_\alpha & G_\alpha & H_\alpha & I_\alpha & J_\alpha & 3-4\nu_s & -1\\ E_\beta & F_\beta & G_\beta & H_\beta & I_\beta & J_\beta & 0 & -1\\ E_\gamma & F_\gamma & G_\gamma & H_\gamma & I_\gamma & J_\gamma & 0 & 0\\ o_1 & o_2 & o_3 & o_4 & o_5 & o_6 & -\frac{2E_s(1-\nu_s)}{(1+\nu_s)} & \frac{E_s}{(1+\nu_s)}\\ q_1 & q_2 & q_3 & q_4 & q_5 & q_6 & -\frac{E_s(1-2\nu_s)}{(1+\nu_s)} & \frac{E_s}{(1+\nu_s)} \end{pmatrix} \begin{pmatrix} A_1(\xi)\\ A_2(\xi)\\ -A_3(\xi)\\ A_4(\xi)\\ A_5(\xi)\\ -A_6(\xi)\\ M_1(\xi)\\ M_2(\xi) \end{pmatrix} = 0 \tag{33}$$

from which, $A_1(\xi)\sim A_5(\xi)$, $M_1(\xi)$ and $M_2(\xi)$ could be expressed in terms of $A_6(\xi)$ as

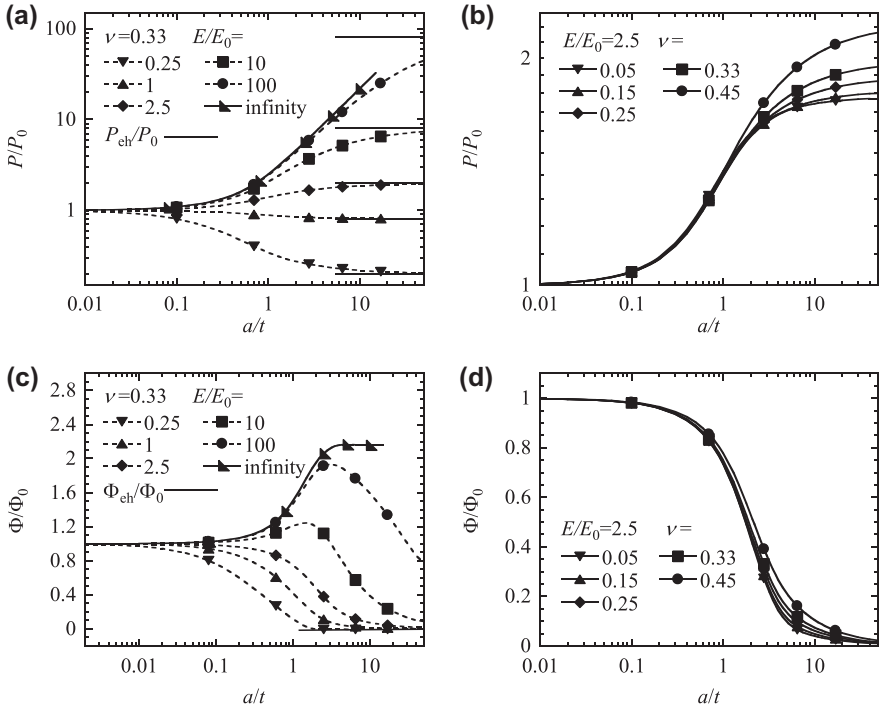

Fig. 2. Normalized insulating punch indentation responses as functions of the normalized contact radius for piezoelectric films bonded to elastic substrates with different moduli and Poisson's ratios: (a) and (b) Indentation force; (c) and (d) Electric potential.

$$[A_1(\xi),A_2(\xi),A_3(\xi),A_4(\xi),A_5(\xi),M_1(\xi),M_2(\xi)]^T = [F_1,F_2,F_3,F_4,F_5,F_6,F_7]^T A_6(\xi)/\Delta, \tag{34}$$

where F_i $(i=1,\ldots,6)$ and Δ are the determinants of the corresponding coefficient matrix according to the Crammer's rule for the solutions of linear equations for which the explicit forms are not given here for the sake of brevity, and the superscript "T" denotes transpose.

Substituting Eq. (34) into Eqs. (25) and (27), we get the following dual integral equations

$$\begin{cases} \sigma_{zz}(r,0) = \int_0^\infty \left(\frac{m_1F_1+m_2F_2-m_3F_3+m_4F_4+m_5F_5}{\Delta} - m_6\right) \\ \qquad A_6(\xi)\xi^2 J_0(\xi r)\mathrm{d}\xi = 0 \quad (r>a), \\ u_z(r,0) = \int_0^\infty \left(\frac{\beta_1F_1+\beta_{21}F_2-\beta_{22}F_3+\beta_3F_4+\beta_{41}F_5}{\Delta} - \beta_{42}\right) \\ \qquad A_6(\xi)\xi J_0(\xi r)\mathrm{d}\xi = h - f(r) \quad (0\leqslant r\leqslant a). \end{cases} \tag{35}$$

For the conducting indenter case, the corresponding equations are

$$\begin{pmatrix} l_1 & l_2 & l_3 & l_4 & l_5 & l_6 & 0 & 0 \\ E_\alpha & F_\alpha & G_\alpha & H_\alpha & I_\alpha & J_\alpha & 3-4\nu_s & -1 \\ E_\beta & F_\beta & G_\beta & H_\beta & I_\beta & J_\beta & 0 & -1 \\ E_\gamma & F_\gamma & G_\gamma & H_\gamma & I_\gamma & J_\gamma & 0 & 0 \\ o_1 & o_2 & o_3 & o_4 & o_5 & o_6 & -\frac{2E_s(1-\nu_s)}{(1+\nu_s)} & \frac{E_s}{(1+\nu_s)} \\ q_1 & q_2 & q_3 & q_4 & q_5 & q_6 & -\frac{E_s(1-2\nu_s)}{(1+\nu_s)} & \frac{E_s}{(1+\nu_s)} \end{pmatrix} \begin{pmatrix} A_1(\xi) \\ A_2(\xi) \\ -A_3(\xi) \\ A_4(\xi) \\ A_5(\xi) \\ -A_6(\xi) \\ M_1(\xi) \\ M_2(\xi) \end{pmatrix} = 0 \tag{36}$$

from which $A_1(\xi)$, $A_2(\xi)$, $A_4(\xi)$, $A_5(\xi)$, $M_1(\xi)$ and $M_2(\xi)$ can be expressed in terms of $A_3(\xi)$ and $A_6(\xi)$ as:

$$[A_1(\xi),A_2(\xi),A_4(\xi),A_5(\xi),M_1(\xi),M_2(\xi)]^T = [F_{c1},F_{c2},F_{c3},F_{c4},F_{c5},F_{c6}]^T \frac{A_3(\xi)}{\Delta_c} + [E_{c1},E_{c2},E_{c3},E_{c4},E_{c5},E_{c6}]^T \frac{A_6(\xi)}{\Delta_c}, \tag{37}$$

where F_{ci}, $E_{ci}(i=1,\ldots,6)$ and Δ_c are the determinants of the corresponding coefficient matrix according to the Crammer's rule.

One set of dual integral equations for the conducting indenter indentation can be obtained from the mechanical boundary conditions (i.e., Eqs. (25) and (27)) as

$$\begin{cases} \sigma_{zz}(r,0) = \int_0^\infty \left[\left(\frac{m_1F_{c1}+m_2F_{c2}+m_4F_{c3}+m_5F_{c4}}{\Delta_c} - m_3\right)A_3(\xi) + \left(\frac{m_1E_{c1}+m_2E_{c2}+m_4E_{c3}+m_5E_{c4}}{\Delta_c} - m_6\right)A_6(\xi)\right]\xi^2 J_0(\xi r)\mathrm{d}\xi = 0 \ (r>a), \\ u_z(r,0) = \int_0^\infty \left[\left(\frac{\beta_1F_{c1}+\beta_{21}F_{c2}+\beta_3F_{c3}+\beta_{41}F_{c4}}{\Delta_c} - \beta_{22}\right)A_3(\xi) + \left(\frac{\beta_1E_{c1}+\beta_{21}E_{c2}+\beta_3E_{c3}+\beta_{41}E_{c4}}{\Delta_c} - \beta_{42}\right)A_6(\xi)\right]\xi J_0(\xi r)\mathrm{d}\xi = h - f(r) \ (0\leqslant r\leqslant a) \end{cases} \tag{38}$$

and another set of dual integral equations from the electric boundary conditions (i.e., Eq. (30)) can be formulated as

$$\begin{cases} D_z(r,0) = \int_0^\infty \left[\left(\frac{n_1F_{c1}+n_2F_{c2}+n_4F_{c3}+n_5F_{c4}}{\Delta_c} - n_3\right)A_3(\xi) + \left(\frac{n_1E_{c1}+n_2E_{c2}+n_4E_{c3}+n_5E_{c4}}{\Delta_c} - n_6\right)A_6(\xi)\right]\xi^2 J_0(\xi r)\mathrm{d}\xi = 0 \ \ (r>a), \\ \phi(r,0) = \int_0^\infty \left(\frac{\gamma_1F_{c1}+\gamma_{21}F_{c2}+\gamma_3F_{c3}+\gamma_{41}F_{c4}}{\Delta_c} - \gamma_{22}\right)A_3(\xi) + \left(\frac{\gamma_1E_{c1}+\gamma_{21}E_{c2}+\gamma_3E_{c3}+\gamma_{41}E_{c4}}{\Delta_c} - \gamma_{42}\right)A_6(\xi)\right]\xi J_0(\xi r)\mathrm{d}\xi = \phi_1 \ \ (0\leqslant r\leqslant a). \end{cases} \tag{39}$$

By now, the key point of the piezoelectric indentation problem is to solve the dual integral Eq. (35) for the insulating case while to solve the dual integral Eqs. (38) and (39) simultaneously for the conducting case.

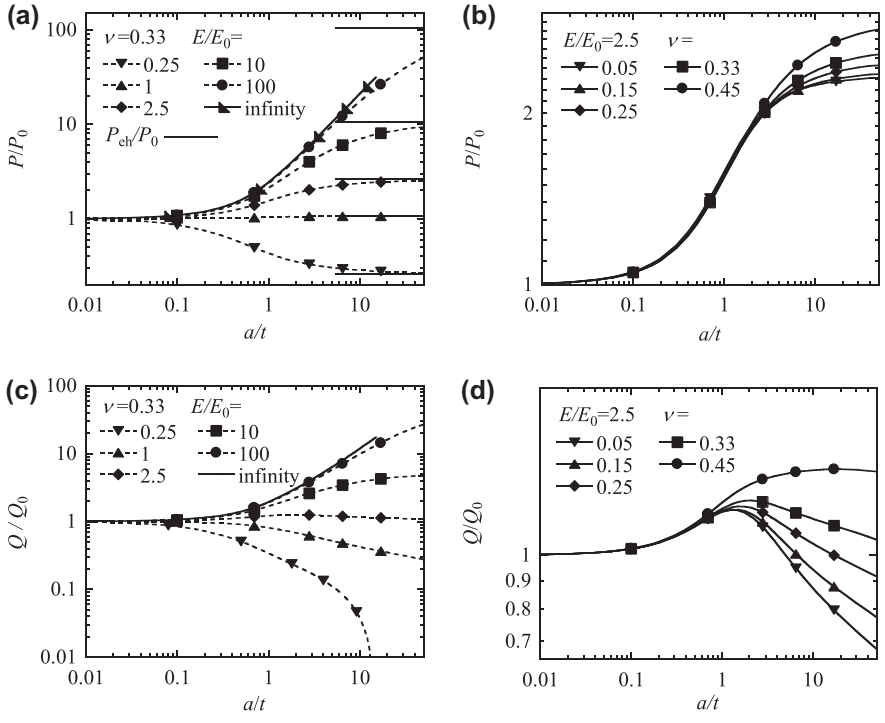

Fig. 3. Normalized conducting punch indentation responses as functions of the normalized contact radius for piezoelectric films bonded to elastic substrates with different moduli and Poisson's ratios: (a) and (b) Indentation force; (c) and (d) Electric charge.

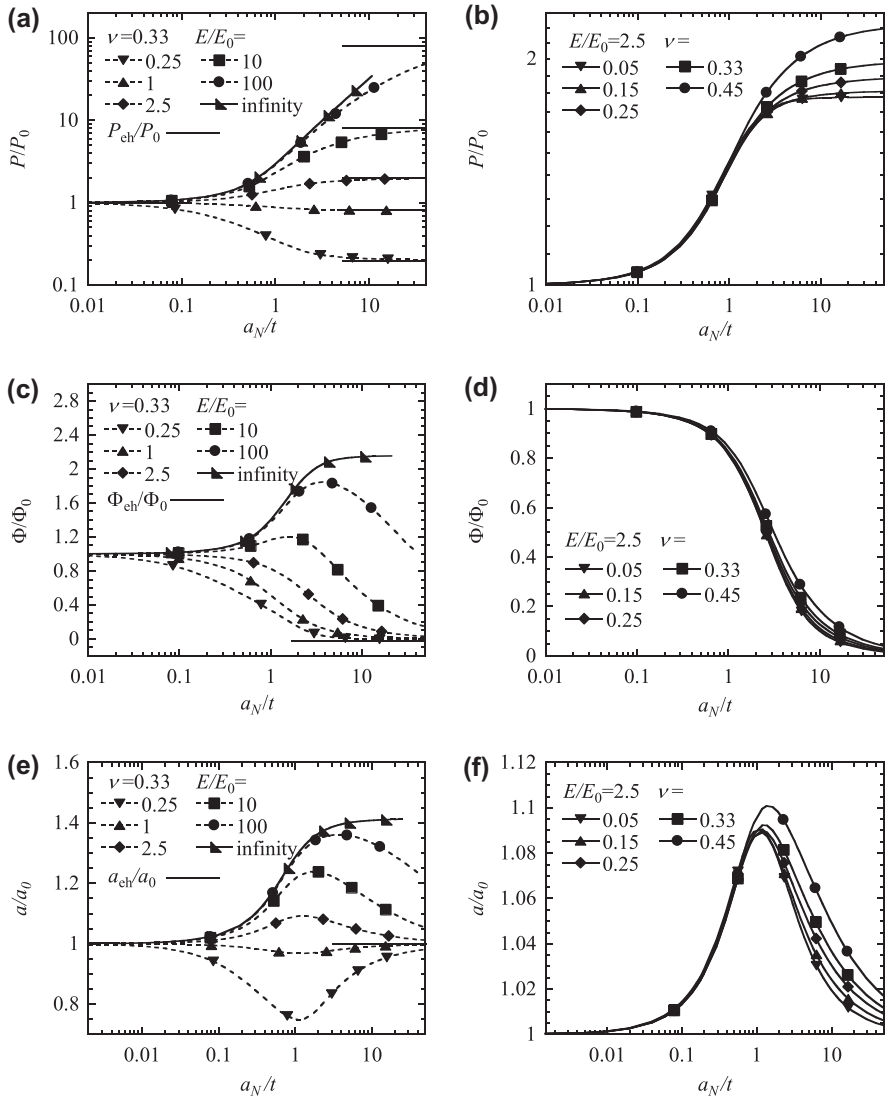

Fig. 4. Normalized insulating spherical indenter indentation responses as functions of the normalized nominal contact radius for piezoelectric films bonded to elastic substrates with different moduli and Poisson's ratios: (a) and (b) Indentation force; (c) and (d) Electric potential; (e) and (f) Contact radius.

3. Solutions for limiting cases

In general, both the film and the half space substrate contribute to the indentation behaviors of a piezoelectric film/elastic substrate system. It is almost impossible to obtain a closed-form solution to the derived dual integral Eqs. (35), (38) and (39). When the contact radius is much smaller than the thickness of the film (i.e., $a \ll t$ or $a/t \to 0$), however, the piezoelectric film can be envisioned as a half-space and the effects of the substrate diminish. As a result, the indentation responses can be approximated by those of a corresponding piezoelectric half space (Giannakopoulos and Suresh, 1999; Wang et al., 2008b).

On the other hand, when the contact radius is much greater than the film thickness (i.e., $a \gg t$ or $a/t \to \infty$) and the Young's modulus of the substrate is finite, the elastic half space substrate dominates the contribution to the response of the film/substrate system to a rigid indenter. Under such a circumstance, it is reasonable to assume that the indenter is directly imposed on the elastic half space substrate. Available solutions of isotropic elastic half space by axisymmetric rigid indenters are summarized in Table 1 (Sneddon, 1951). It should be pointed out that there only exist force and contact radius responses for an isotropic elastic half space and all the electric indentation responses (i.e., electric potential for an insulating indenter indentation and electric charge for a conducting case) are zero (see, Table 1). This will be viewed from the numerical results in the following section. When the Young's modulus of the substrate increases to infinity (i.e., rigid substrate), the indentation responses should converge to the infinitely thin film solutions bonded to rigid substrate given by Wang et al. (2008b). Details will be discussed in the following.

4. Numerical results

4.1. Specifications

Since the focus of this study is to explore the effects of the thickness of the piezoelectric film and the elasticity of the substrate on the indentation responses, systematical numerical calculations are conducted by solving the dual integral Eqs. 35, 38 and 39 using the same method as that in Wang et al. (2008b). The material properties listed in Table 2 for the piezoelectric ceramic PZT-4 are adopted unless stated otherwise.

In the following, the calculated indentation responses are normalized by the corresponding ones of piezoelectric half space for

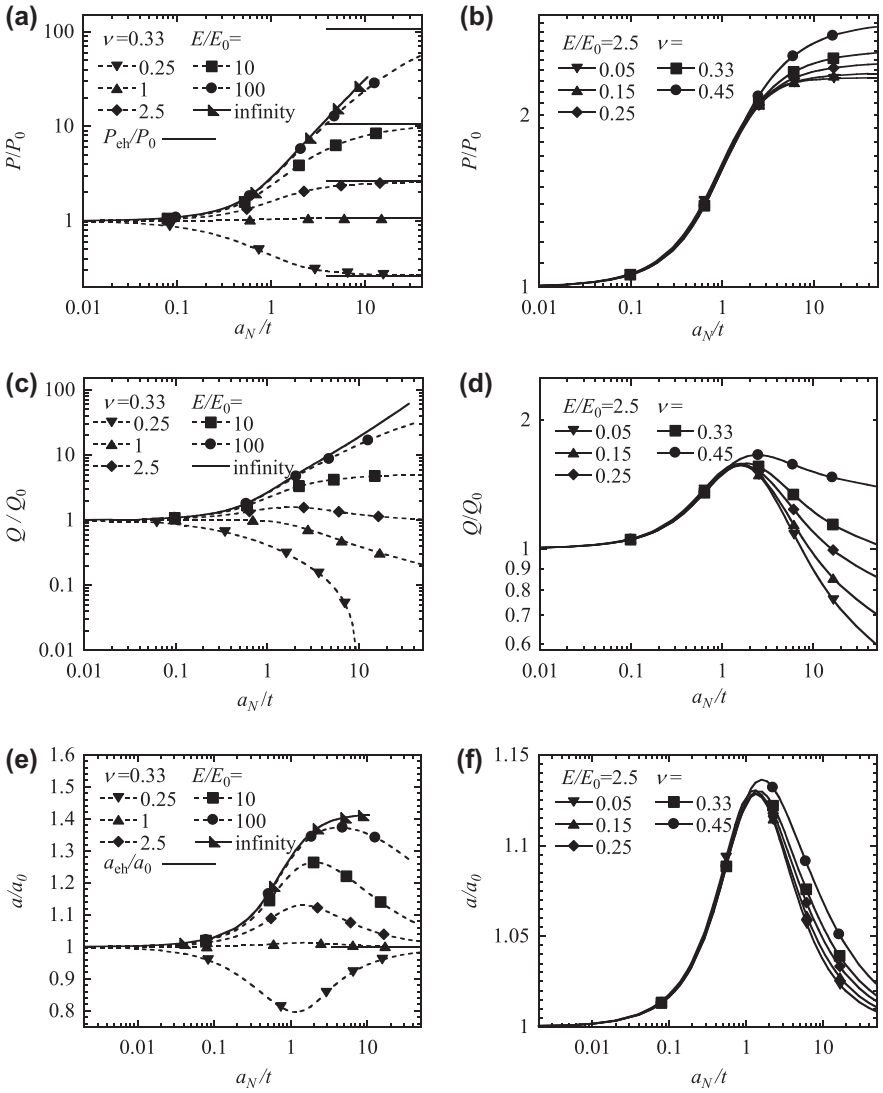

Fig. 5. Normalized conducting spherical indenter indentation responses as functions of the normalized nominal contact radius for piezoelectric films bonded to elastic substrates with different moduli and Poisson's ratios: (a) and (b) Indentation force; (c) and (d) Electric charge; (e) and (f) Contact radius.

a better illustration of the film thickness effect. Specifically, the calculated force P, electric potential $\Phi = \phi(0,0)$, electric charge Q, and indentation radius a are normalized by the corresponding piezoelectric half space solutions P_0, $\Phi_0 = \phi_0(0,0)$, Q_0 and a_0 given in Tables 1 and 2 of Wang et al. (2008b), that is,

$$P/P_0, \quad \Phi/\Phi_0, \quad Q/Q_0, \quad a/a_0. \tag{40}$$

It is therefore expected that as $a/t \to 0$

$$(P/P_0,\ \Phi/\Phi_0,\ Q/Q_0,\ a/a_0) \to (1,\ 1,\ 1,\ 1). \tag{41}$$

For $a/t \to \infty$, as discussed before, the corresponding indentation responses should approach the isotropic elastic half space solutions (i.e., results given in Table 1), that is

$$(P/P_0,\ \Phi/\Phi_0,\ Q/Q_0,\ a/a_0) \to (P_{eh}/P_0,\ 0,\ 0,\ 1), \tag{42}$$

where the subscript "*eh*" denotes the elastic half-space.

For a transversely isotropic piezoelectric film, its Young's modulus E_0 and Poisson's ratio v_0 in the isotropic plane are related to its elastic constants by

$$\begin{cases} E_0 = \frac{c_{11}^2 c_{33} - 2c_{11}c_{13}^2 - c_{12}^2 c_{33} + 2c_{12}c_{13}^2}{c_{11}c_{33} - c_{13}^2}, \\ v_0 = \frac{c_{12}c_{33} - c_{13}^2}{c_{11}c_{33} - c_{13}^2}, \end{cases} \tag{43}$$

which gives $E_0 = 81.2$ GPa and $v_0 = 0.33$ for PZT-4. To illustrate the effects of the elastic substrate, numerical calculations are conducted for various Young's moduli and Poisson's ratios of the substrate. Specifically, when the Poisson's ratio is the selected values of 0.33, the Young's modulus of the substrate is set to be 20GPa, 81.2 GPa, 200 GPa, 812 GPa and 8120 GPa, respectively, which means that the corresponding mismatch effect E_s/E_0 is set to be 0.25, 1, 2.5, 10, and 100. Furthermore, to explore the effects of the Poisson's ratio, the Young's modulus of the substrate is fixed to be 200 GPa while the Poisson's ratio is set to be 0.05, 0.15, 0.25, 0.33 and 0.45.

For the conical and spherical indenter indentations, a nominal contact radius a_N is introduced

$$a_N = \begin{cases} h\tan\Theta & \text{(cone)}, \\ \sqrt{hR} & \text{(sphere)} \end{cases} \tag{44}$$

and $\Theta = 70.3^\circ$ for cone and $R/t = 1000$ for sphere have been selected. The prescribed electric voltage of $\phi_1/t = 10^4$V/m is assumed

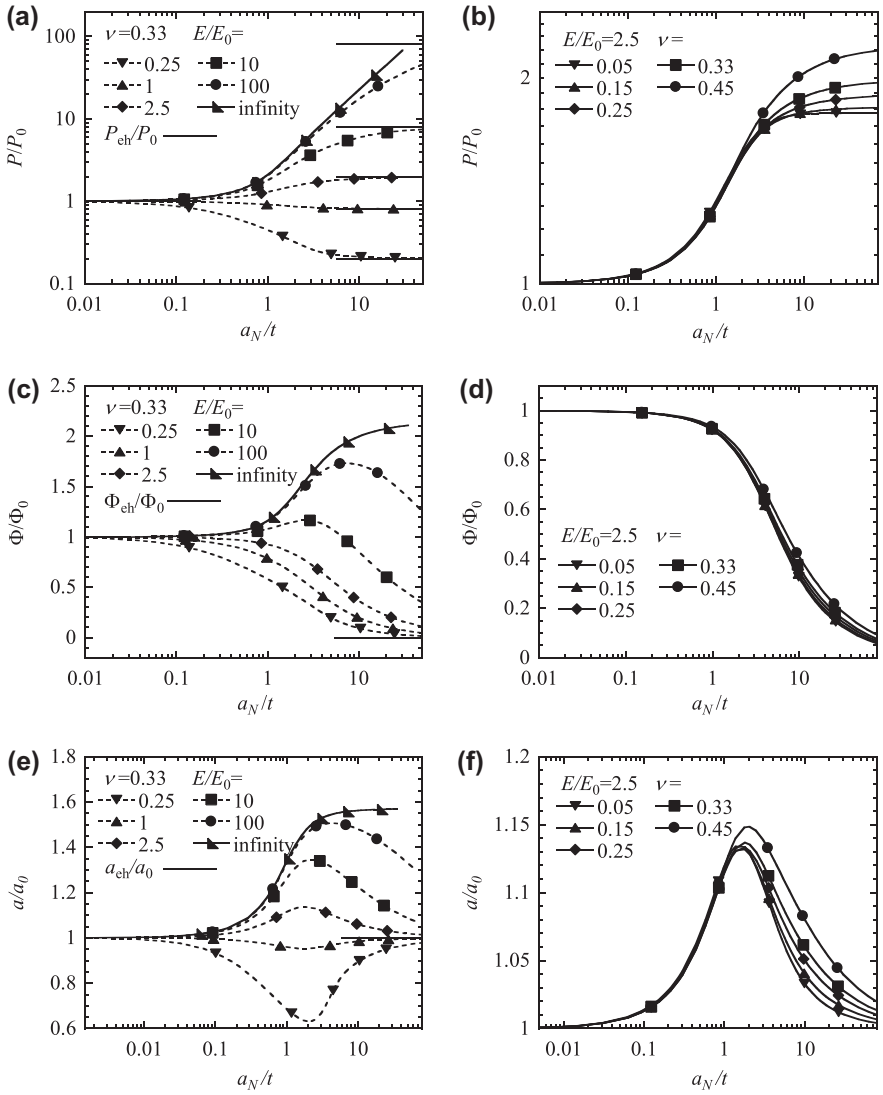

Fig. 6. Normalized insulating conical indenter indentation responses as functions of the normalized nominal contact radius for piezoelectric films bonded to elastic substrates with different moduli and Poisson's ratios: (a) and (b) Indentation force; (c) and (d) Electric potential; (e) and (f) Contact radius.

for the conducting indenter cases. Note that for the cylindrical punch indentation, the normalized indentation depth h/t remains constant and is chosen to be 0.1 during the calculation.

4.2. Results

The calculated indentation responses of finitely thin piezoelectric films bonded to elastic substrates with different Young's moduli and Poisson's ratios and loaded by an insulating or conducting punch, sphere and cone are shown in Figs. 2–7, respectively. All the results are given in terms of normalized responses versus normalized contact radius a/t or a_N/t and denoted by dotted lines with symbols. The corresponding results for the rigid substrate (Wang et al., 2008b) are also included and shown as solid lines with symbols and the normalized elastic half space results are plotted in solid lines without symbols.

Recall that in the two limiting cases of $a/t \to 0$ (for cone and sphere, a/t should be a_N/t) and $a/t \to \infty$, the indentation responses of the piezoelectric film/elastic substrate system should approach those of piezoelectric half space and elastic half space, respectively. It is evident from Figs. 2–7 that all the solutions get to unity as $a/t \to 0$, indicating that the effects of the elastic substrate in this limit case disappear and the system could be regarded as a piezoelectric half space. As a/t increases, the calculated responses gradually change into the corresponding elastic half space results.

Comparing Figs. 2 and 3(a), Figs. 4 and 5(e), the electric conductivity of the indenter (i.e., ideally insulating or conducting) is found to have little influences on the mechanical responses, such as the force and contact radius responses, but produces different indentation electric responses, i.e., electric potential for the insulating indentations (see, Fig. 2(c)) and electric charge for the conducting indentations (see, Fig. 3(c)). The force, electric potential and electric charge responses for the three types of indenters (i.e., cylindrical punch, sphere and cone) and the contact radius responses for the two types of indenters (i.e., sphere and cone) are almost the same only with minor difference (see, Figs. 2–7).

However, the influences of the Young's modulus and Poisson's ratio of the substrate on the indentation responses are significant and they are discussed in detail as follows.

The influence of the Young's modulus of the elastic substrate

It is seen from the plot (a) of Figs. 2–7 that the indentation forces responses for both conducting and insulating indenters switch from the piezoelectric to the elastic half space solutions as the contact radius increases from small to big values, independent of

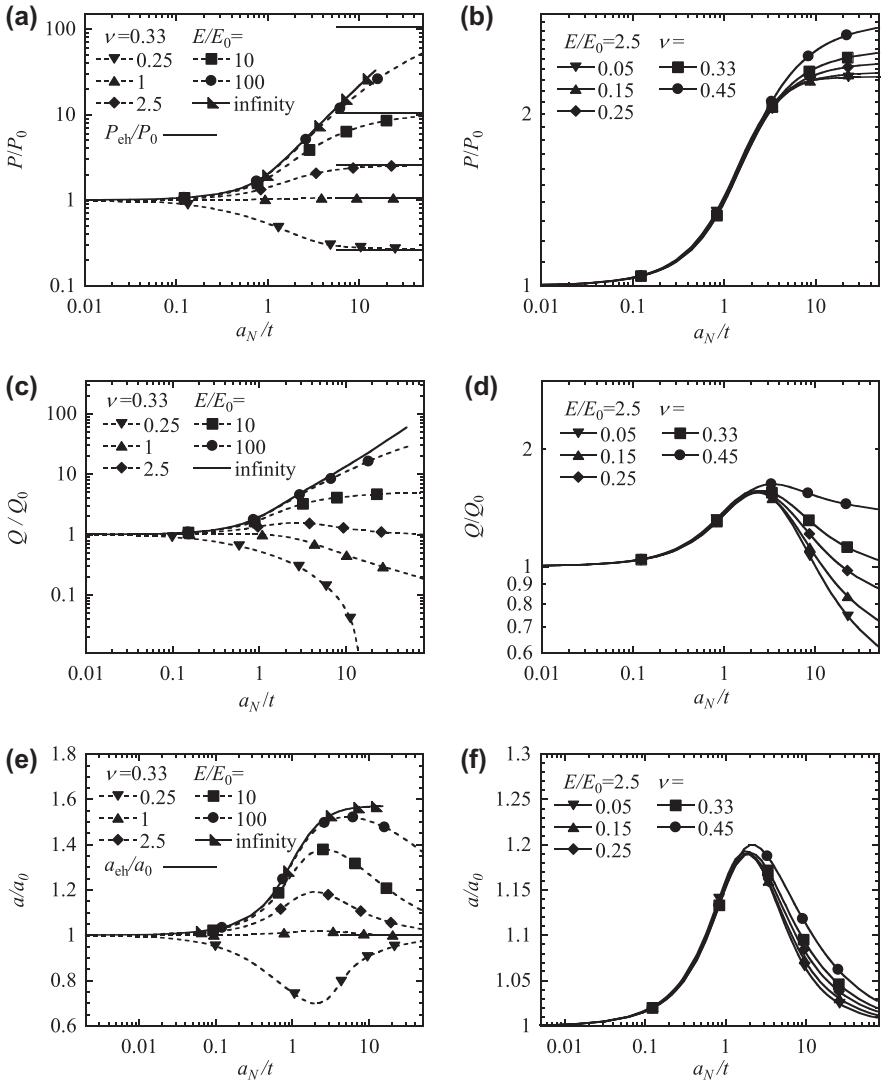

Fig. 7. Normalized conducting conical indenter indentation responses as functions of the normalized nominal contact radius for piezoelectric films bonded to elastic substrates with different moduli and Poisson's ratios: (a) and (b) Indentation force; (c) and (d) Electric charge; (e) and (f) Contact radius.

whether the substrate is soft or hard. The transition occurs around $a/t = 1$ (or $a_N/t = 1$). Specifically, when the Young's modulus of the substrate is small (e.g., $E/E_0 = 0.25$, that is the case of a hard film on a soft substrate), the plot (a) of Figs. 2–7 shows that the normalized indentation force responses are below 1 and decrease gradually to P_{eh}/P_0 while for the case of a soft film on a hard substrate (e.g., $E/E_0 = 2.5$), they are above 1 and increase gradually to the normalized elastic half space results. As the Young's modulus E gets larger, the corresponding responses approach the rigid substrate solutions although it becomes more and more difficult for the indentation force to get to P_{eh}/P_0 as a/t increases.

For the normalized contact radius responses of the conducting and insulating spherical and conical indenters (see, plots (e) and (f) of Figs. 4–7), since a_{eh}/a_0 is very close to 1 (if not exactly equal to 1) regardless of the Young's modulus of the substrate, they approach 1 as a/t increases. In particular, for $E/E_0 = 0.25$, they reduce from 1 first and then increase gradually to a_{eh}/a_0 while for $E/E_0 = 2.5$ they rise up first and then decreases to 1. For very large Young's modulus of the substrate (e.g., $E/E_0 = 100$), a/a_0 is very closed to the rigid substrate solution when $a/t < 1$. For larger a/t, it deviates from the rigid substrate solution and drops down toward the elastic half space results. It can be seen that, for the Young's modulus close to E_0, it is relatively easy (i.e., $a/t = 10$) for the mechanical indentation responses (i.e., force and contact radius) to approach the elastic half space results.

The influences of the Young's modulus of the substrate on the electric responses (i.e., electric potential for the insulating indenter case and electric charge for the conducting indenter case) are different from those on the indentation force and contact radius responses. From the plot (c) of Figs. 2, 4 and 6, it is seen that the electric potential responses decrease from the half space results gradually to zero, that is Φ_{eh}/Φ_0, as a/t varying from 0.01 to a large value for even $E/E_0 = 2.5$. The smaller E/E_0, the quicker the normalized responses decrease to Φ_{eh}/Φ_0. For larger Young's moduli (e.g., $E/E_0 > 2.5$), the electric potential increases first and then decrease to 0 even at $E/E_0 = 100$ similar to the behaviors of the contact radius responses and it does change into the rigid substrate electric potential response as $E/E_0 \to \infty$. For the electric charge responses, see plot (c) of Figs. 2, 3, 5 and 7, they decrease first slowly and then dramatically to 0, i.e., Q_{eh}/Q_0, as a/t increases for $E/E_0 = 0.25$, indicating that for the case of indentation for a hard film on a soft substrate, the electrical charge responses may vanish at a special value of a/t which is determined by the elasticity of the substrate. For larger Young's moduli of the substrate (i.e.,

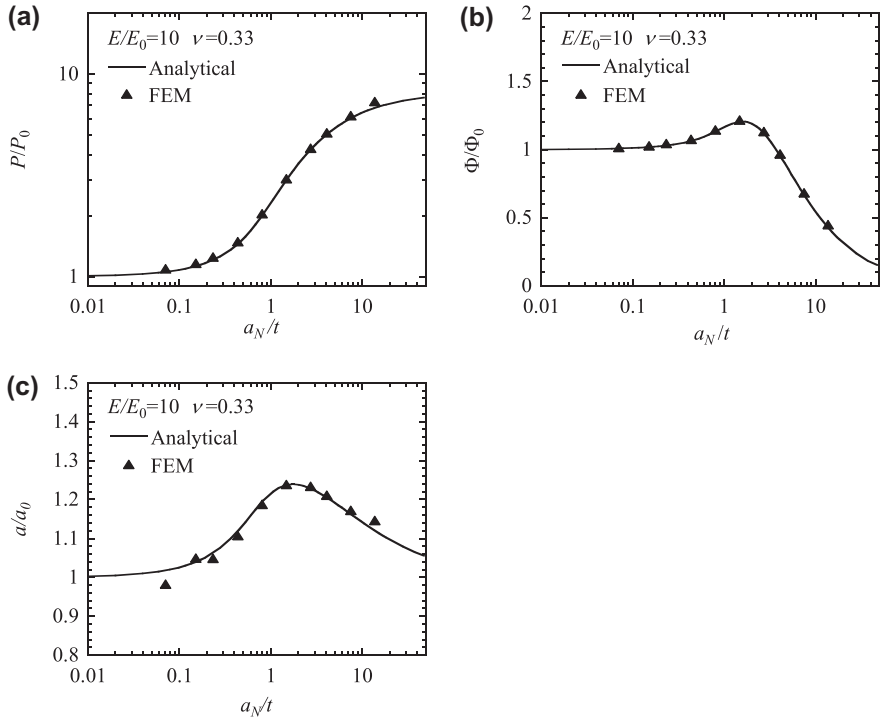

Fig. 8. Comparison of the calculated responses of the insulating spherical indenter case with the finite element results: (a) Force; (b) Electric potential; (c) Contact radius.

$E/E_0 \geqslant 10$), the normalized indentation electric charge increase without a sign of dropping down within the range of a/t considered in this paper, similar to the behaviors of the indentation force responses. As $E/E_0 \to \infty$, it is found that the electric charge responses turn to the rigid substrate solutions.

As mentioned in Section 3, the indentation responses of a film on substrate system comprise contributions from the piezoelectric film and the elastic substrate. It is evident from the Figs. 2–7 that all the responses transfer from the corresponding piezoelectric half space results to the elastic substrate solutions as a/t varies from small to big values, indicating that when a/t is small the contribution from the piezoelectric film dominates and the contribution from the elastic substrate increases and even prevails as a/t gets significantly larger. The transition point between film dominated and substrate dominated is closely related to the Young's modulus and Poisson's ratio of the elastic substrate.

As a rule of thumb, the ratio of the contact radius to the film thickness should be less than one tenth to diminish the influences of the substrate on the indentation responses. As a consequence, the piezoelectric film/elastic substrate system can be simplified as a piezoelectric half space. However, this rule must be used with caution. Although it is true (see, Figs. 2–7) for a substrate with large Young's modulus (e.g., $E/E_0 = 2.5$), it may not be so obvious for a hard film bonded to a soft substrate (e.g., $E/E_0 = 0.25$): the calculated indentation responses are different from the piezoelectric half space solutions even at a small value of $a/t = 0.1$, which means that the system cannot be simplified as a piezoelectric half space. For a soft film bonded to a hard substrate case (i.e., $E/E_0 \geqslant 2.5$), there are evident discrepancy between the calculated responses and the rigid substrate solutions for $a/t = 1$ and $E/E_0 = 10$, implying that the substrate may be deemed as rigid only when $E/E_0 > 10$ and $a/t < 1$.

The influences of the Poisson's ratio of the elastic substrate

One can see from Figs. 2–7 that, when $a/t < 1$, the influences of the Poisson's ratio of the substrate on all the normalized indentation responses are small. However, the influences are significant for $a/t > 1$ that the bigger the Poisson's ratio of the elastic substrate, the larger the corresponding indentation responses are. We can conclude that there is no need to consider the influences of Poisson's ratio of the substrate for a normalized indentation with $a/t < 1$ while for $a/t \geqslant 1$ the influences must be taken into account.

4.3. Finite element verification

To verify the analytical calculations in previous sections, a finite element analysis using the software ABAQUS is conducted on the indentation of a piezoelectric film bonded to an elastic substrate and penetrated by an insulating spherical indenter. The Young's modulus and Poisson's ratio of the isotropic elastic substrate are set to be 812GPa and 0.33, respectively whilst the transversely isotropic piezoelectric film is PZT4 with the material properties listed in Table 2. The film with the thickness 0.016 mm is ideally bonded to the substrate. Quadratic axisysmetric elements CAX8RE and CAX8R are adopted to model the film and substrate, respectively, and an analytical rigid spherical surface is used for the spherical indenter with radius 16mm, giving the ratio of the sphere radius to the film thickness being 1000. There are 400 elements in the r direction and 200 in the z direction with 5 for the piezoelectric film. The total number of degrees of freedom of the finite element model is about 0.8 million.

The finite element calculated indentation responses, such as the indentation force, electric potential and contact radius, are compared with the corresponding analytical solutions given in previous sections (see, Fig. 8). Good agreement between the finite element and analytical results can be observed, indicating the validity of the obtained analytical solutions.

5. Concluding remarks

We conduct a systematical study on the frictionless indentation responses of a piezoelectric film perfectly bonded to an elastic sub-

strate using the integral transform method. Derived analytical results are validated by the finite element method. Three different geometrical rigid indenters, i.e., circular cylindrical punch, cylindrical cone, and sphere, both perfectly insulating and conducting are considered.

Obtained results on the effects of the film thickness reveal that in the two limit cases of the contact radius to the film thickness ratio the considered problems can be simplified: For a/t or $a_N/t \to 0$, the effects of the substrate can be neglected and the problems can be deemed as the indentations of piezoelectric half space; For a/t or $a_N/t \to \infty$, on the other hand, the indentation responses of the film/substrate system transfer to those of the elastic half space solutions.

The influences of the elasticity of the substrate on the indentation force, electric potential, electric charge and contact radius responses are explored by assigning various sets of Young's modulus and Poisson's ratio to the substrate. As the normalized contact radius a/t (or a_N/t) varies from small to big values, the indentation force response switches monotonically from the piezoelectric half space solution to the elastic half space solution, regardless whether the substrate is soft or hard. The transition takes place at around a/t=1 (or a_N/t=1). For the contact radius, electric potential and electric charge responses, however, the transition from the piezoelectric to the elastic half space solutions are much more complicated and are dependent upon whether the substrate is soft or hard. In particular, the electric charge response of insulating indenters first decreases slowly and then drops down dramatically to zero for very soft substrate, indicating that the electric charge responses may disappear for a special value of a/t. When the Young's modulus of the substrate increases to infinity (i.e., rigid substrate), all the calculated responses converges into the available solutions for piezoelectric film/rigid substrate systems. The effects of the Poisson's ratio on the indentation responses are found to be negligible for small values of normalized contact radius. The results are believed to be useful for developing experimental techniques to extract the material properties of the piezoelectric film/substrate system.

Acknowledgements

The authors are grateful for the financial support of this work by the National Natural Science Foundation of China (Nos. 11072127 and 10832002) and by the National Basic Research Program of China (No. 2011CB610305).

Appendix A

The definitions for l_i, m_i, n_i, o_i, q_i $(i = 1, \ldots 6)$ are

$$\begin{aligned}
l_1 &= -e_{15}\gamma_1 - c_{44}(k_1\alpha_1 + \beta_1),\\
l_2 &= -e_{15}\gamma_{21} - c_{44}(\delta\alpha_{21} - \omega\alpha_{22} + \beta_{21}),\\
l_3 &= -e_{15}\gamma_{22} - c_{44}(\delta\alpha_{22} + \omega\alpha_{21} + \beta_{22}),\\
l_4 &= -e_{15}\gamma_3 - c_{44}(-k_1\alpha_3 + \beta_3),\\
l_5 &= -e_{15}\gamma_{41} - c_{44}(-\delta\alpha_{41} + \omega\alpha_{42} + \beta_{41}),\\
l_6 &= -e_{15}\gamma_{42} - c_{44}(-\delta\alpha_{42} - \omega\alpha_{41} + \beta_{42}),
\end{aligned} \tag{A1}$$

$$\begin{aligned}
m_1 &= \alpha_1 c_{13} - c_{33}\beta_1 k_1 - e_{33}\gamma_1 k_1,\\
m_2 &= \alpha_{21} c_{13} - c_{33}\beta_{21}\delta + c_{33}\beta_{22}\omega - e_{33}\gamma_{21}\delta + e_{33}\gamma_{22}\omega,\\
m_3 &= \alpha_{22} c_{13} - c_{33}\beta_{22}\delta - c_{33}\beta_{21}\omega - e_{33}\gamma_{22}\delta - e_{33}\gamma_{21}\omega,\\
m_4 &= \alpha_3 c_{13} + c_{33}\beta_3 k_1 + e_{33}\gamma_3 k_1,\\
m_5 &= \alpha_{41} c_{13} + c_{33}\beta_{41}\delta - c_{33}\beta_{42}\omega + e_{33}\gamma_{41}\delta - e_{33}\gamma_{42}\omega,\\
m_6 &= \alpha_{42} c_{13} + c_{33}\beta_{42}\delta + c_{33}\beta_{41}\omega + e_{33}\gamma_{42}\delta + e_{33}\gamma_{41}\omega,
\end{aligned} \tag{A2}$$

$$\begin{aligned}
n_1 &= \alpha_1 e_{31} - e_{33}\beta_1 k_1 + \in_{33}\gamma_1 k_1,\\
n_2 &= \alpha_{21} e_{31} - e_{33}\beta_{21}\delta + e_{33}\beta_{22}\omega + \in_{33}\gamma_{21}\delta - \in_{33}\gamma_{22}\omega,\\
n_3 &= \alpha_{22} e_{31} - e_{33}\beta_{22}\delta - e_{33}\beta_{21}\omega + \in_{33}\gamma_{22}\delta + \in_{33}\gamma_{21}\omega,\\
n_4 &= e_{31}\alpha_3 + e_{33}\beta_3 k_1 - \in_{33}\gamma_3 k_1,\\
n_5 &= \alpha_{41} e_{31} + e_{33}\beta_{41}\delta - e_{33}\beta_{42}\omega - \in_{33}\gamma_{41}\delta + \in_{33}\gamma_{42}\omega,\\
n_6 &= \alpha_{42} e_{31} + e_{33}\beta_{42}\delta + e_{33}\beta_{41}\omega - \in_{33}\gamma_{42}\delta - \in_{33}\gamma_{41}\omega,
\end{aligned} \tag{A3}$$

$$\begin{aligned}
o_1 &= l_1 e^{-k_1\xi t};\\
o_2 &= (l_2\cos(w\xi t) + l_3\sin(w\xi t))e^{-\delta\xi t};\\
o_3 &= (l_3\cos(w\xi t) - l_2\sin(w\xi t))e^{-\delta\xi t};\\
o_4 &= l_4 e^{k_1\xi t};\\
o_5 &= (l_5\cos(w\xi t) - l_6\sin(w\xi t))e^{\delta\xi t};\\
o_6 &= (l_6\cos(w\xi t) + l_5\sin(w\xi t))e^{\delta\xi t};
\end{aligned} \tag{A4}$$

$$\begin{aligned}
q_1 &= m_1 e^{-k_1\xi t};\\
q_2 &= (m_2\cos(w\xi t) + m_3\sin(w\xi t))e^{-\delta\xi t};\\
q_3 &= (m_3\cos(w\xi t) - m_2\sin(w\xi t))e^{-\delta\xi t};\\
q_4 &= m_4 e^{k_1\xi t};\\
q_5 &= (m_5\cos(w\xi t) - m_6\sin(w\xi t))e^{\delta\xi t};\\
q_6 &= (m_6\cos(w\xi t) + m_5\sin(w\xi t))e^{\delta\xi t};
\end{aligned} \tag{A5}$$

The definitions for $E_\alpha, F_\alpha, G_\alpha, H_\alpha, I_\alpha, J_\alpha$ are:

$$\begin{aligned}
E_\alpha &= \alpha_1 e^{-k_1\xi\tilde{t}},\\
F_\alpha &= (\alpha_{21}\cos(\omega\xi\tilde{t}) + \alpha_{22}\sin(\omega\xi\tilde{t}))e^{-\delta\xi\tilde{t}},\\
G_\alpha &= (\alpha_{22}\cos(\omega\xi\tilde{t}) - \alpha_{21}\sin(\omega\xi\tilde{t}))e^{-\delta\xi\tilde{t}},\\
H_\alpha &= \alpha_3 e^{k_1\xi\tilde{t}},\\
I_\alpha &= (\alpha_{41}\cos(\omega\xi\tilde{t}) - \alpha_{42}\sin(\omega\xi\tilde{t}))e^{\delta\xi\tilde{t}},\\
J_\alpha &= (\alpha_{42}\cos(\omega\xi\tilde{t}) + \alpha_{41}\sin(\omega\xi\tilde{t}))e^{\delta\xi\tilde{t}}.
\end{aligned} \tag{A6}$$

And replacing α here into β and γ gives the definitions for $E_\beta \sim J_\beta$ and $E_\gamma \sim J_\gamma$.

References

Bahr, D.F., Robach, J.S., Wright, J.S., Francis, L.F., Gerberich, W.W., 1999. Mechanical deformation of PZT thin films for MEMS applications. Mater. Sci. Eng. A-Struct. 259, 126–131.

Birk, H., Glatz-Reichenbach, J., Jie, L., et al., 1991. The local piezoelectric activity of thin polymer films observed by scanning tunneling microscopy. J. Vac. Sci. Technol. B 9, 1162–1165.

Busby, J.T., Hash, M.C., Was, G.S., 2005. The relationship between hardness and yield stress in irradiated austenitic and ferritic steels. J. Nucl. Mater. 336, 267–278.

Chen, W.Q., Ding, H.J., 1999. Indentation of a transversely isotropic piezoelectric half-space by a rigid sphere. Acta. Mech. Sol. Sin 12, 114–120.

Chen, W.Q., Shioya, T., Ding, H.J., 1999. The elasto-electric field for a rigid conical punch on a transversely isotropic piezoelectric half-space. ASME J. Appl. Mech. 66, 764–771.

Chen, S., Liu, L., Wang, T., 2005. Investigation of the mechanical properties of thin films by nanoindentation, considering the effects of thickness and different coating-substrate combinations. Surf. Coat. Tech. 191, 25–32.

Chen, Z.R., Yu, S.W., 2005. Micro-scale adhesive contact of a spherical rigid punch on a piezoelectric half-space. Comp. Sci. Tech. 65, 1372–1381.

Christman, J.A., Woolcott, R.R., Kingon, A.I., Nemanich, R.J., 1998. Piezoelectric measurements with atomic force microscopy. Appl. Phys. Lett. 73, 3851.

Delobelle, P., Guillon, O., Fribourg-Blanc, E., Soyer, C., Cattan, E., Remiens, D., 2004. True Young modulus of Pb(Zr,Ti)O^3 films measured by nanoindentation. Appl. Phys. Lett. 85, 5185–5187.

Ding, H.J., Hou, P.F., Gou, F.L., 2000. The elastic and electric fields for three dimensional contact for transversely isotropic piezoelectric materials. Int. J. Solids Struct. 37, 3201–3229.

Doerner, M.F., Nix, W.D., 1986. A method for interpreting the data from depth-sensing indentation instruments. J. Mater. Res. 1, 601–609.

Gao, H., Chiu, C.H., Lee, J., 1992. Elastic contact versus indentation modeling of multi-layered materials. Int. J. Solids Struct. 29, 2471–2492.

Gao, Y.F., Xu, H.T., Oliver, W.C., Pharr, G.M., 2008. Effective elastic moduli of film-on-substrate systems under normal and tangential contact. J. Mech. Phys. Solids 56, 402–416.

Giannakopoulos, A.E., Suresh, S., 1999. Theory of indentation of piezoelectric materials. Acta. Mater. 47, 2153–2164.

Johnson, K.L., 1985. Contact Mechanics. Cambridge University press, Cambridge, UK.

Kalinin, S.V., Karapetian, E., Kachanov, M., 2004. Nanoelectromechanics of piezoresponse force microscopy. Phys. Rev. B 70, 18401–18424.
King, R.B., 1987. Elastic analysis of some punch problems for a layered medium. Int. J. Solids Struct. 23, 1657–1664.
Karapetian, E., Kachanov, M., Sevostianov, I., 2002. The principle of correspondence between elastic and piezoelectric problems. Arch. Appl. Mech. 72, 564–587.
Karapetian, E., Kachanov, M., Kalinin, S.V., 2009. Stiffness relations for piezoelectric indentation of flat and non-flat punches of arbitrary planform: applications to probing nanoelectromechanical properties of materials. J. Mech. Phys. Solids 57, 673–688.
Mason, W.P., 1950. Piezoelectric Crystals and their Application to Ultrasonics. Van Nostrand Reinhold, New York, USA.
Matysiak, S., 1985. Axisymmetric problem of punch pressing into a piezoelectroelastic half space. Bull. Pol. Acad. Sci. Tech. 33, 25–34.
Mencik, J., Munz, D., Quandt, E., Weppelmann, E.R., Swain, M.V., 1997. Determination of elastic moduli of thin layers using nanoindentation. J. Mater. Res. 12, 2475–2484.
Ning, X.G., Michael, L., William, S., 2006. Asymptotic solutions for axisymmetric contact of a thin, transversely isotropic elastic layer. Wear 260, 693–698.
Oliver, W.C., Pharr, G.M., 1992. An improved technique for determining hardness and elastic modulus using load and displacement sensing indentation experiments. J. Mater. Res. 7, 1564–1583.
Oliver, W.C., Pharr, G.M., 2004. Measurement of hardness and elastic modulus by instrumented indentation: advances in understanding and refinements to methodology. J. Mater. Res. 19, 3–20.
Ramamurty, U., Sridhar, S., Giannakopoulos, A.E., Suresh, S., 1999. An experimental study of spherical indentation on piezoelectric materials. Acta Mater. 47, 2417–2430.
Rar, A., Pharr, G.M., Oliver, W.C., Karapetian, E., Kalinin, S.V., 2006. Piezoelectric nanoindentation. J. Mater. Res. 21, 552–556.
Saha, R., Nix, W.D., 2002. Effects of the substrate on the determination of thin film mechanical properties by nanoindentation. Acta Mater. 50, 23–38.
Sridhar, S., Giannakopoulos, A.E., Suresh, S., Ramamurty, U., 1999. Electric responses during indentation of piezoelectric materials: a new method for material characterization. J. Appl. Phys. 85, 385–387.
Uchino, K., 1997. Piezoelectric Actuators and Ultrasonic Motors. Kluwer Academic Publishers, Boston, Dordrecht, London.
Wang, B.B.L., Han, J.C., Du, S.Y., Zhang, H.Y., Sun, Y.G., 2008a. Electromechanical behavior of a finite piezoelectric layer under a flat punch. Int. J. Solids Struct. 45, 6384–6398.
Wang, B.L., Han, J.C., 2006. A circular indenter on a piezoelectric layer. Arch. Appl. Mech. 76, 367–379.
Wang, J.G., Fang, S.S., Chen, L.F., 2002. The state vector methods for space axisymmetric problems in multilayered piezoelectric media. Int. J. Solids Struct. 39, 3959–3970.
Wang, J.H., Chen, C.Q., Lu, T.J., 2008b. Indentation responses of piezoelectric films. J. Mech. Phys. Solids 56, 3331–3351.
Wang, Z.K., Zheng, B.L., 1995. The general solution of three-dimensional problem in piezoelectric media. Int. J. Solids Struct. 32, 105–120.
Yang, F., 2003. Thickness effect on the indentation of an elastic layer. Mater. Sci. Eng. A-Struct. 358, 226–232.
Yang, F.Q., 2008. Analysis of the axisymmetric indentation of a semi-infinite piezoelectric material: The evaluation of the contact stiffness and the effective piezoelectric constant. J. Appl. Phys. 103, 074115–074122.
Yu, H.Y., 2001. A concise treatment of indentation problems in transversely isotropic half-spaces. Int. J. Solids Struct. 38, 2213–2232.
Zavala, G., Fendler, J.H., Trolier-McKinstry, S., 1997. Characterization of ferroelectric lead zirconate titanate films by scanning force microscopy. J. Appl. Phys. 81, 7480–7491.
Zhao, M.H., Wang, Z.L., Mao, S.X., 2004. Piezoelectric Characterization of Individual Zinc Oxide Nanobelt Probed by Piezoresponse Force Microscope. Nano. Lett. 4, 587–590.
Zheng, X.J., Zhou, Y.C., Li, J.Y., 2003. Nano-indentation fracture test of Pb(Zr0.25Ti0.48)O3 ferroelectric thin films. Acta Mater. 51, 3985–3997.